▮ Electro, Physical & Theoretical Chemistry

Are Small Quasi-Fullerenes Capable of Encapsulating Trimetallic Nitrides $A_{3-x}B_xN$ (A, B = Sc, Y, La, x = 0-3)? A DFT Study

Christian A. Celaya,*[a] Miguel Reina,[a] Jesús Muñiz,[b, c] and Luis Enrique Sansores[a]

The capacity of small quasi-fullerenes (C_{48-q} and C_{60-q}, q stands for quasi) to encapsulate trimetallic nitride clusters; $A_{3-x}B_xN$ (A, B=Sc, Y, La, x = 0-3) was investigated by applying Density Functional Theory (DFT). Optimized geometries and the computation of ΔG formation energies, $\Delta E_{HOMO-LUMO}$ energy values, chemical potential, chemical hardness and aromaticity were all performed in order to understand chemical reactivity and thermal stability of these novel quasi-metallofullerenes. Moreover, the donor-acceptor properties of the quasi-metal-lofullerenes systems compared to the bare quasi-fullerene cages are also analyzed. Finally, to understand the effect of temperature at which quasi-fullerenes could be subjected to, *ab initio* molecular dynamics (MD) was also performed. The main conclusion of this report is that small quasi-fullerenes are capable of encapsulating trimetallic nitride clusters, and that the donor-acceptor properties are enhanced due to the presence of clusters.

Introduction

Soon after the discovery of C_{60} fullerene by Kroto et al.,[1] the idea of encapsulating atoms, ions or molecules became popular since the hollow carbon-closed cages could serve as versatile containers for other systems.[2–20] The presence of metal transition compounds inside different types of fullerenes enhances the stability and donor-acceptor properties.[21–25] These systems are called endohedral metallofullerenes, characterized by a charge transfer from the encapsulated metal atoms to the carbon cage.[21–26] The discovery of metal nitride cluster fullerenes in 1999 opened the gate for the synthesis of carbon cages with cluster species inside. Neither the trimetallic nitride cluster nor the C_{80} fullerene of icosahedral symmetry has been obtained separately. However, if combined, they can form a system with a very high stability.[4] Trimetallic nitride clusters (A_3N, A = group III, IV, and rare-earth) have been studied as guest compounds in fullerenes due to their high stability and electronic and magnetic properties.[27–32] Today, an important variety of trimetallic nitride encapsulated fullerenes have been synthesized, as reported by Zhang et al.[25] To this regard, Density Functional Theory (DFT) calculations have predicted the formation of these compounds through charge transfer from the trimetallic nitride clusters to the carbon cages.[21,24] Some of these systems have been proposed as versatile biomedical, semiconductor, optoelectronic, and light electron/energy conversion materials.[5,33–39] Furthermore, quasi-fullerenes are a family type of fullerenes characterized by a spherical closed structure composed of pentagons and hexagons combined with rings of different sizes.[40–43] In general, they are less stable than fullerenes and more difficult to isolate.[44–46] As a consequence, the study of these systems at the theoretical level has become essential to fully understand their stability and their chemical properties.[47–51] Quasi-fullerenes present a very complex and diverse molecular topography and they are particularly interesting since they present a larger diameter compared to their analogous fullerenes. In spite of all the information gathered so far, the theoretical study of the possible encapsulation of trimetallic scandium, yttrium and lanthanum nitrides and their mixed clusters in small quasi-fullerenes has not been investigated. This could be interesting since the relatively small quasi-fullerenes (C_{48-q} and C_{60-q}) could allocate large trimetallic nitrides clusters, and thus modify chemical stability and donor-acceptor properties. Additionally, the stabilization of these quasi-fullerenes could be enhanced by the presence of trimetallic nitrides clusters. Consequently, it may be possible to isolate such systems. The aim of this theoretical work is to investigate if small C_{48} and C_{60} quasi-fullerenes are capable of encapsulating trimetallic nitrides (A_3N and $A_{3-x}B_xN$, A, B= Sc, Y and La and x = 0-3) with favorable structural configurations. The effect of temperature at which quasi-fullerenes could be subjected to, has also been explored by using *ab initio* molecular dynamics (MD). We also examined the donor-acceptor properties of quasi-fullerene systems with

[a] C. A. Celaya, Dr. M. Reina, Prof. L. E. Sansores
Departamento de Materiales de Baja Dimensionalidad
Instituto de Investigaciones en Materiales
Universidad Nacional Autónoma de México
Circuito Exterior S.N. Ciudad Universitaria, Apartado postal 70–360, Coy-oacán C.P. 04510, Ciudad de México, México
E-mail: acelaya@iim.unam.mx

[b] Dr. J. Muñiz
Instituto de Energías Renovables
Universidad Nacional Autónoma de México
Priv. Xochicalco s/n, Col. Centro, CP 62580, Temixco, Morelos, México

[c] Dr. J. Muñiz
CONACYT-Universidad Nacional Autónoma de México
Priv. Xochicalco s/n, Col. Centro, CP 62580, Temixco, Morelos, México

Figure 1. Schematic representation of quasi-fullerenes C_{48-q} and C_{60-q}.

Results and discussion

Geometry Optimization

Figure 1 shows a schematic representation of quasi-fullerenes C_{48-q} and C_{60-q}, (q stands for quasi).

Ground state geometries of A_3N and $A_{3-x}B_xN$ (A, B = Sc, Y, La, $x = 0$-3) clusters are depicted on Figure 2. All clusters have a pyramidal geometry with the nitrogen atom in the center. The point group symmetry is C_{3v} for A_3N systems and C_s for all the other trimetallic nitride clusters.

For the initial geometries, we placed the trimetallic nitride cluster in the center of the quasi-fullerenes (C_{48-q} and C_{60-q}). Figures 3 and 4 show the optimized structures of $A_3N@C_{n-q}$ and $A_{3-x}B_xN@C_{n-q}$ (A, B= Sc, Y, La, $x = 0$-3 and $n = 48$ and 60). In all cases, interaction distances (Å) between the cluster and the carbon cage are reported for comparison purposes. In Figure 3, we report the optimized geometries for the $A_3N@C_{48-q}$ and $A_{3-x}B_x@C_{48-q}$ systems. As apparent in the Figure 3, all trimetallic nitride clusters can be encapsulated by the small quasi-fullerene C_{48-q}. The only exception is $La_2N@C_{48-q}$-La, where the

most stable geometry corresponds to the dissociation of trimetallic nitride cluster. As shown in Figure 3, one La atom is on the surface of the quasi-fullerene. This singularity could be attributed to the larger size of La_3N cluster compared to the other trimetallic nitride clusters. In Figure 4, we report the optimized geometries for the $A_3N@C_{60-q}$ and $A_{3-x}B_x@C_{60-q}$ systems. In all cases, the most stable structure corresponds to the cluster inside the C_{60-q} carbon cage. As expected, N–Sc distances are shorter than N–Y and N–La, respectively. As previously reported,[52,53] the change of shape (3D to planar) may be important to stabilize these kinds of systems. In endohedral fullerenes, planar structures undergo a free rotation in the carbon cage, thus the charge transfer is more effective, and the system becomes more stable.[52–55]

The ΔG energy values are reported on Figure 5 for the encapsulation reaction of trimetallic nitride clusters and quasi-fullerenes. Negative values indicate that the reaction is exergonic and consequently, thermodynamically viable. In all analyzed cases, the ΔG energy values are negative, indicating that C_{48-q} and C_{60-q} systems are capable of encapsulating the trimetallic nitride cluster under study. Particularly, in the case of the C_{48-q} molecule, it can be observed that as the cluster size increases, the capacity of the quasi-fullerene to encapsulate the trimetallic nitride compound decreases. As another criterion to assess stability, we computed atomization energies in accordance to Eq. 4 (see Computational methods of Supporting Information). For practically all endohedral systems of $@C_{48-q}$ studied, atomization energy is less stable than the bare quasi-fullerene cage (exceptions: $Sc_3N@C_{48-q}$, $YSc_2N@C_{48-q}$ and $ScY_2N@C_{48-q}$, see Fig. SM2 of Supporting Information). In accordance to atomization energies, trimetallic nitride clusters inside the quasi-fullerene $@C_{60-q}$ are more stable than the bare quasi-fullerene cage.
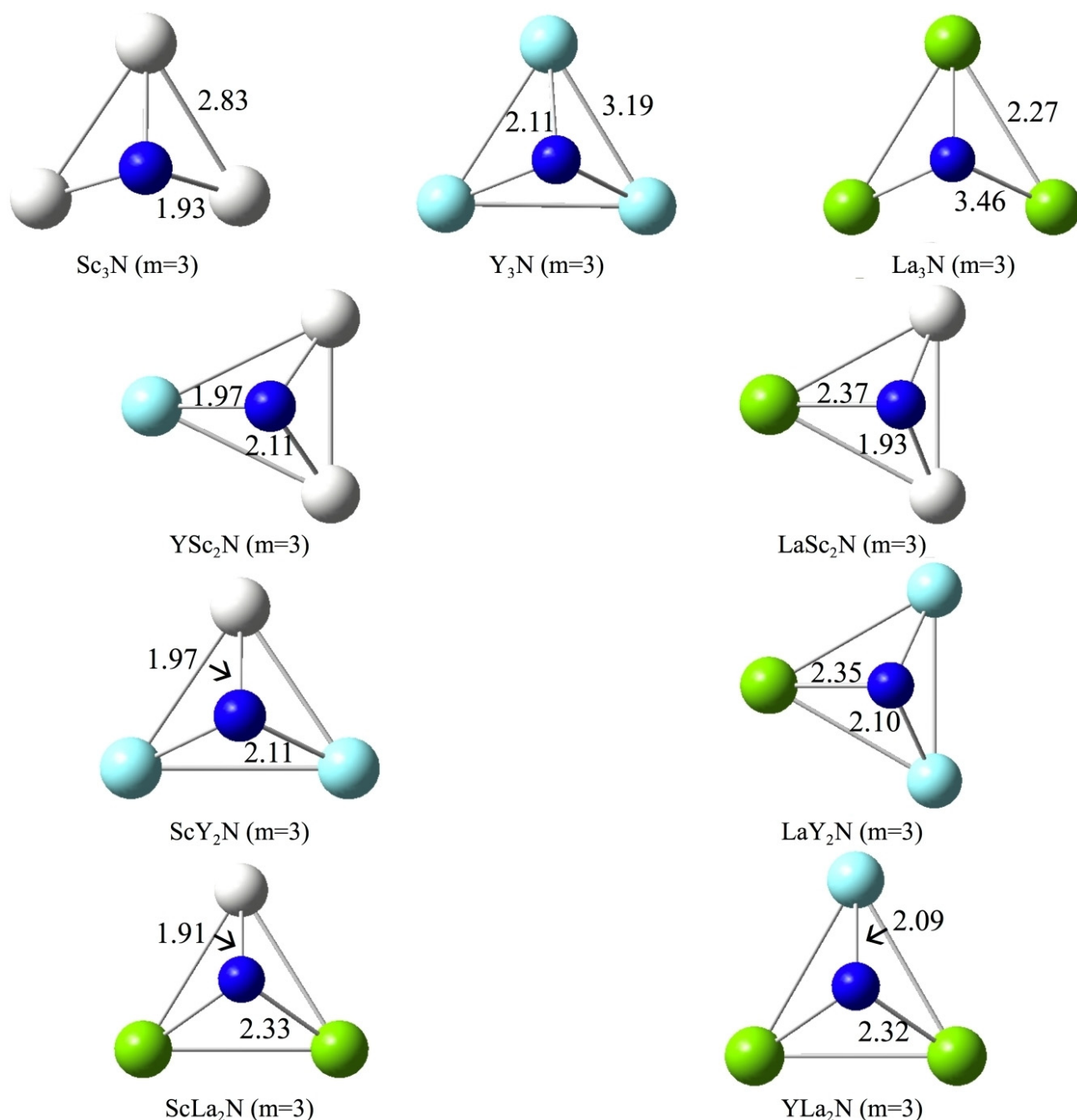
trimetallic nitrides compared to those without clusters. As apparent in this report, most of small quasi-fullerenes are capable of encapsulating trimetallic nitride systems. The ratio of quasi-fullerene and cluster size is crucial to understand the capacity to encapsulate different species, especially for the smallest quasi-fullerene analyzed, C_{48-q}. Additionally, the donor-acceptor properties of systems containing trimetallic nitrides are slightly enhanced compared to those without clusters. These molecular systems could have potential application as antioxidant materials, electronic devices or new nanomaterial with the capacity to store energy and further experimental studies may also be done in this direction.

Figure 2. Optimized geometries of A_3N and $A_{3-x}B_xN$ (A,B= Sc, Y, La, x=0-3) clusters. Bond distances (in Å) are also indicated. Color code atom: N (blue), Sc (white), Y (turquoise) and La (green).

The more exergonic reaction corresponds to the smallest cluster (Sc$_3$N@C$_{48-q}$, $\Delta G = -9.0$ eV). For the C$_{60-q}$ system, the size of the cluster appears as not to be determinant for the capacity to encapsulate. In all cases, the C$_{60-q}$ quasi-fullerene is capable of encapsulating the trimetallic nitride clusters with similar ΔG energy values. The reaction with highest thermodynamically viability corresponds to the formation of the YLa$_2$N@C$_{60-q}$ compound ($\Delta G = -10.1$ eV) and the reaction with lowest viability corresponds to the encapsulation of LaY$_2$N@C$_{60-q}$ ($\Delta G=$

-8.0 eV). For all systems under study, C$_{60-q}$ presents more negative values than C$_{48-q}$, and thus, the capacity to encapsulate the trimetallic nitride cluster is thermodynamically increased.

Chemical stability

Chemical stability of the encapsulated compounds has also been studied by considering some electronic structure proper-
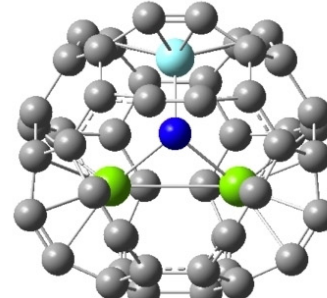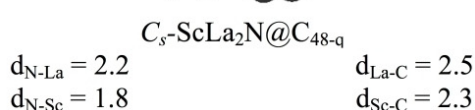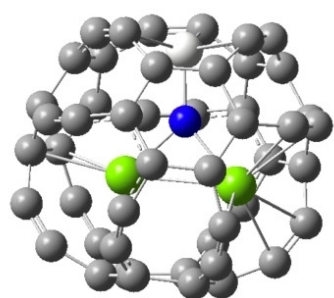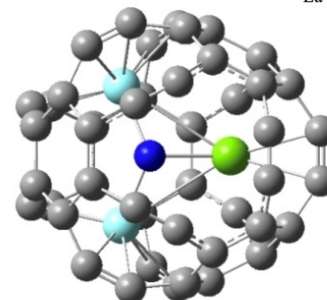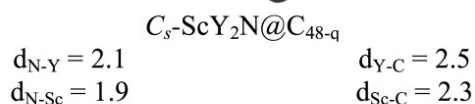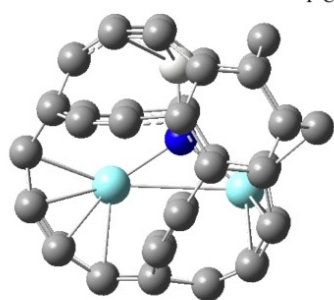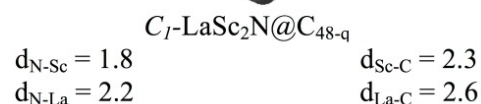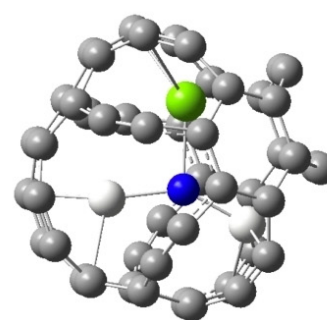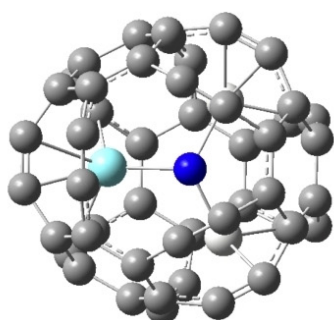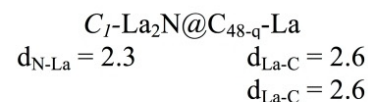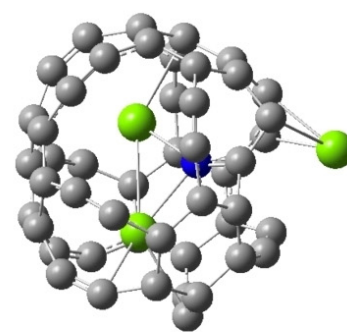
Figure 3. Optimized geometries of $A_3N@C_{48-q}$ and $A_{3-x}B_xN@C_{48-q}$. Interaction distances (in Å) are indicated for each system. Color code atom: C (gray), N (blue), Sc (white), Y (turquoise) and La (green).

C_1-$Sc_3N@C_{48-q}$
$d_{N-Sc} = 2.0$ $d_{Sc-C} = 2.3$

C_s-$Y_3N@C_{48-q}$
$d_{N-Y} = 2.1$ $d_{Y-C} = 2.4$

C_1-$La_2N@C_{48-q}$-La
$d_{N-La} = 2.3$ $d_{La-C} = 2.6$
$d_{La-C} = 2.6$

C_1-$YSc_2N@C_{48-q}$
$d_{N-Sc} = 1.9$ $d_{Sc-C} = 2.3$
$d_{N-Y} = 2.1$ $d_{Y-C} = 2.5$

C_1-$LaSc_2N@C_{48-q}$
$d_{N-Sc} = 1.8$ $d_{Sc-C} = 2.3$
$d_{N-La} = 2.2$ $d_{La-C} = 2.6$

C_s-$ScY_2N@C_{48-q}$
$d_{N-Y} = 2.1$ $d_{Y-C} = 2.5$
$d_{N-Sc} = 1.9$ $d_{Sc-C} = 2.3$

C_1-$LaY_2N@C_{48-q}$
$d_{N-Y} = 2.0$ $d_{Y-C} = 2.4$
$d_{N-La} = 2.2$ $d_{La-C} = 2.6$

C_s-$ScLa_2N@C_{48-q}$
$d_{N-La} = 2.2$ $d_{La-C} = 2.5$
$d_{N-Sc} = 1.8$ $d_{Sc-C} = 2.3$

C_1-$YLa_2N@C_{48-q}$
$d_{N-La} = 2.2$ $d_{La-C} = 2.6$
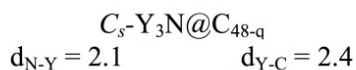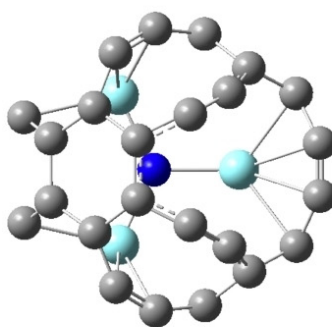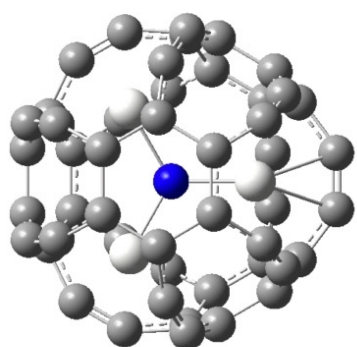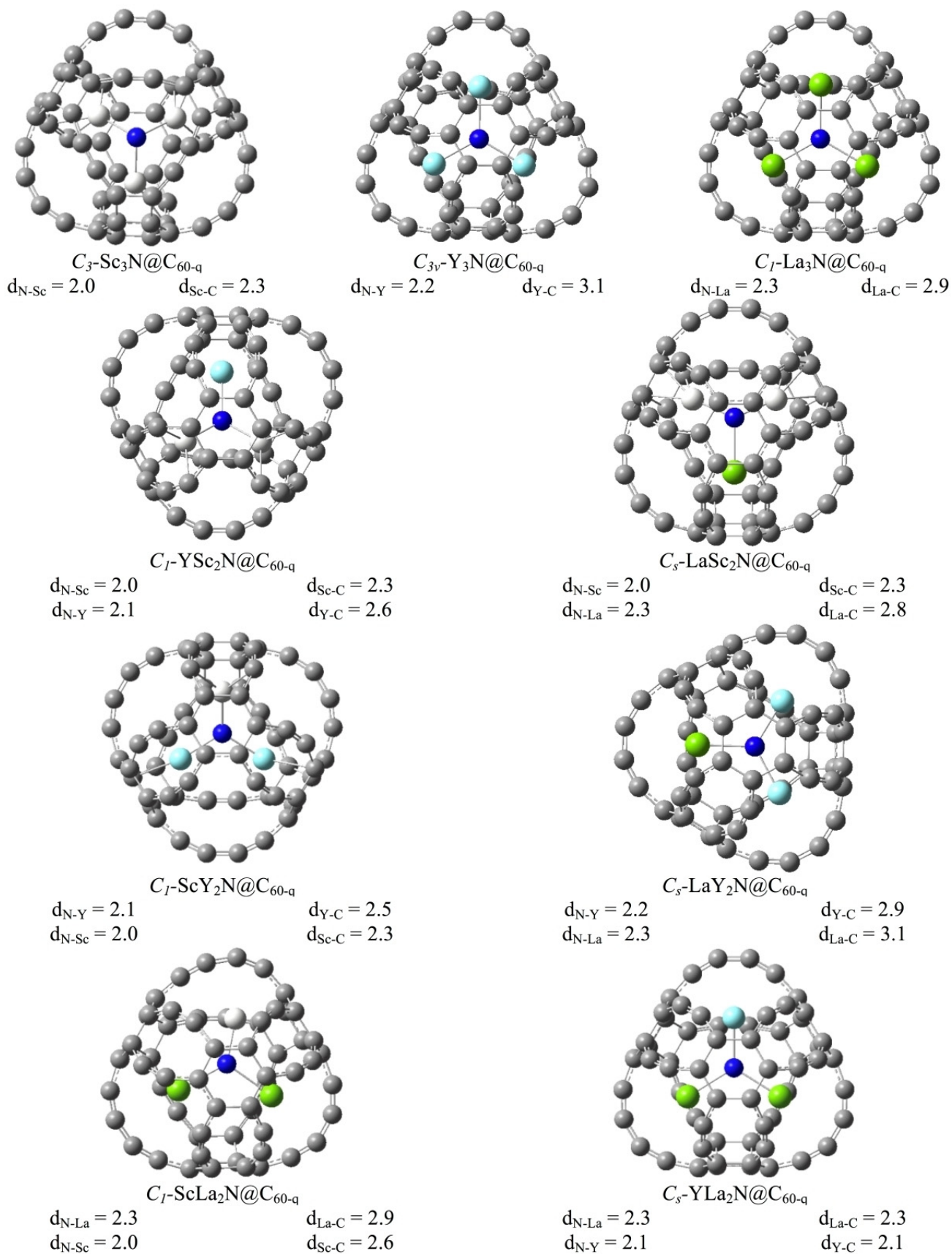$d_{N-Y} = 2.0$ $d_{Y-C} = 2.4$

Figure 4. Optimized geometries of $A_3N@C_{60-q}$ and $A_{3-x}B_xN@C_{60-q}$. Interaction distances (in Å) are indicated for each system. Color code atom: C (gray), N (blue), Sc (white), Y (turquoise) and La (green).
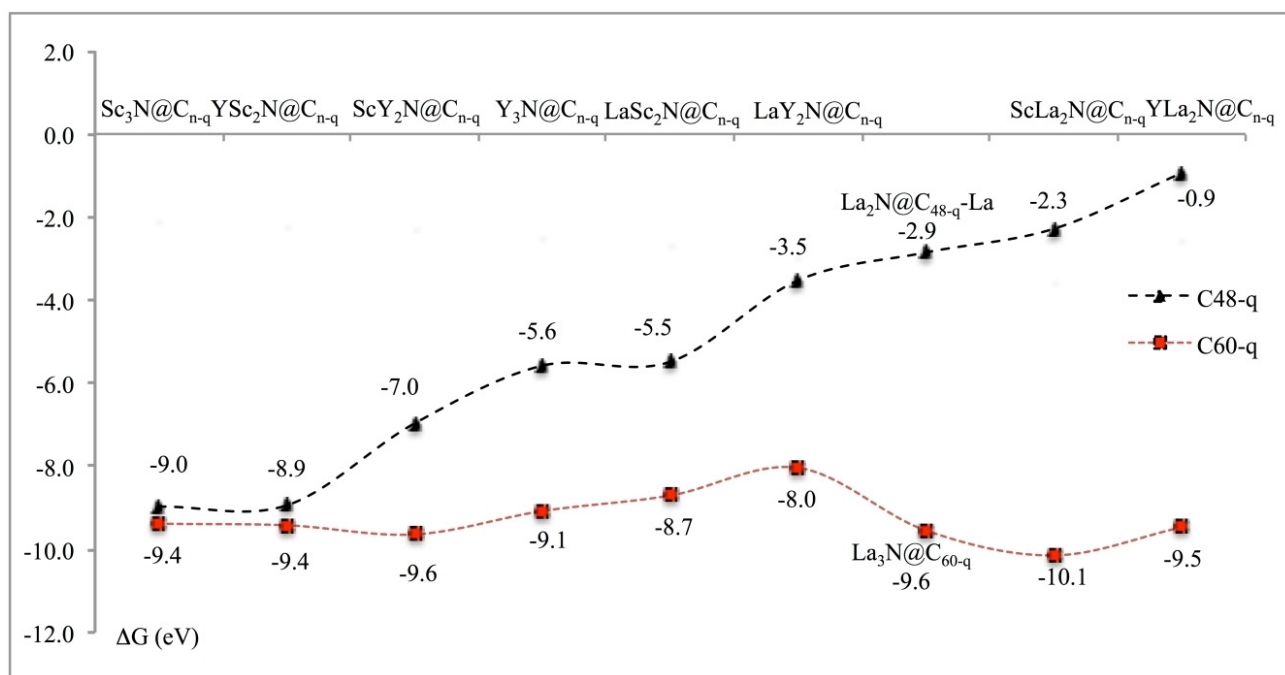
Figure 5. ΔG energy values for $A_3N + C_{n-q} \rightarrow A_3N@C_{n-q}$ and $A_{3-x}B_xN + C_{n-q} \rightarrow A_{3-x}B_xN@C_{n-q}$ reactions.

Molecular system	$\Delta E_{HOMO-LUMO}$ (eV)		μ (eV)		η (eV)	
	C_{48-q}	C_{60-q}	C_{48-q}	C_{60-q}	C_{48-q}	C_{60-q}
$Sc_3N@C_{n-q}$	0.45	0.88	-4.9	-5.0	1.79	1.83
$Y_3N@C_{n-q}$	0.70	0.90	-4.9	-4.8	1.89	1.86
$La_3N@C_{60-q}$	-	0.69	-	-4.7	-	1.74
$YSc_2N@C_{n-q}$	0.42	0.84	-4.9	-4.9	1.77	1.84
$LaSc_2N@C_{n-q}$	0.81	0.78	-4.9	-4.8	1.96	1.80
$ScY_2N@C_{n-q}$	0.71	0.73	-4.9	-4.9	1.91	1.77
$LaY_2N@C_{n-q}$	0.44	0.71	-5.0	-4.7	1.76	1.76
$ScLa_2N@C_{n-q}$	0.67	0.53	-4.9	-4.6	1.88	1.66
$YLa_2N@C_{n-q}$	0.32	0.64	-5.0	-4.7	1.70	1.72
$La_2N@C_{48-q}$-La	0.23	-	-4.4	-	1.64	-
C_{48-q}	1.35	-	-5.2	-	2.27	-
C_{60-q}	-	0.58	-	-5.2	-	1.69

Table 1. Energy gaps ($\Delta E_{HOMO-LUMO}$, eV), chemical potential (μ, eV) and chemical hardness (η, eV).

ties, such as the HOMO-LUMO energy gap ($\Delta E_{HOMO-LUMO}$), chemical potential (μ) and chemical hardness (η).

The presence of trimetallic nitride clusters inside C_{48-q} decreases the HOMO-LUMO energy gap ($\Delta E_{HOMO-LUMO}$ C_{48-q} = 1.35 eV, and $\Delta E_{HOMO-LUMO}$ $A_{3-x}B_xN@C_{48-q}$ ranges from 0.23 to 0.81 eV). $La_2N@C_{48-q}$-La is the system with the lowest energy gap and $LaSc_2@C_{48-q}$ presents the highest energy gap. The decrease of $\Delta E_{HOMO-LUMO}$ for all species formed, give us information about the reactive character of the endohedral quasi-fullerenes (@C_{48-q} and @C_{60-q}). The encapsulation of trimetallic clusters in C_{48-q} decreases also the chemical hardness values. According to the chemical hardness, $La_2N@C_{48-q}$-La is the system with the smallest hardness of the C_{48-q} systems. This is in agreement with it ΔG and atomization energy, and thus this system corresponds to one of the least stable molecules. Contrarily, $LaSc_2@C_{48-q}$ corresponds to the system with the

largest hardness, which is also related to the ΔG and atomization energy found. Following these results, it may be concluded that the $A_{3-x}B_xN@C_{48-q}$ compounds are less stable than the C_{48-q} system. On the contrary, the $A_{3-x}B_xN@C_{60-q}$ systems are more stable than C_{60-q} bare cage and thus, these systems are thermodynamically stable. $Sc_3N@C_{60-q}$ presents the larger hardness value and is a stable system according to the atomization energy (see Fig. SM2 of Supporting Information).

The bare quasi-fullerenes have the same μ. For both quasi-fullerenes studied, C_{48-q} and C_{60-q} the presence of trimetallic nitride clusters decreases the chemical potential. Furthermore, the decrease on chemical potential may be indicative of an electrostatic interaction between cage and trimetallic nitride clusters.[54–56]

NICS(0) and the NICS(1) values are reported on Table 2. NICS(0) were computed at the center of the quasi-fullerene

Table 2. NICS(0) and NICS(1) values.

Molecular system	NICS(0) (ppm)		NICS(1) (ppm)				NICS(1) (ppm)				NICS(1) (ppm)			
	C_{48-q}	C_{60-q}	C_{48-q}		C_{60-q}		C_{48-q}		C_{60-q}		C_{48-q}		C_{60-q}	
Direction (± x,y,z)	-	-	-x	x	-x	x	-y	y	-y	y	-z	z	-z	z
$Sc_3N@C_{n-q}$	204.4	133.3	-26.6	-1.6	-40.3	-31.7	-19.7	-19.5	-34.1	-39.1	-0.6	-23.6	-30.7	-31.8
$Y_3N@C_{n-q}$	-6.7	30.1	-38.8	-34.0	-39.0	-27.3	-36.6	-36.6	-38.5	-39.0	-28.7	-28.7	-27.6	-25.9
$La_3N@C_{60-q}$	-	340.4	-	-	-34.6	-39.9	-	-	-44.6	-28.8	-	-	-31.4	-38.0
$YSc_2N@C_{n-q}$	-64.1	91.8	-4.4	-29.0	-13.8	-41.3	-23.9	-25.7	-37.2	-37.2	-19.8	-12.7	-29.9	-30.4
$LaSc_2N@C_{n-q}$	-41.0	-16.2	-57.3	-23.1	2.8	-40.2	-40.7	-32.5	-29.5	-29.5	-29.2	-29.1	-31.4	-37.6
$ScY_2N@C_{n-q}$	-26.7	103.5	-35.2	-35.4	-25.4	-25.4	-30.7	-49.4	-32.3	-45.5	-28.7	-28.7	-29.0	-31.1
$LaY_2N@C_{n-q}$	3.7	-50.5	-21.8	-19.2	-19.3	-49.3	-30.7	-21.8	-40.4	-40.4	-18.5	-14.1	-35.2	-30.2
$ScLa_2N@C_{n-q}$	-31.1	-16.7	-28.2	-62.5	-24.8	-24.9	-26.1	-1.3	-32.4	-18.6	-25.3	-25.3	-27.2	-35.3
$YLa_2N@C_{n-q}$	-11.2	62.8	0.7	0.7	-30.5	-30.5	-6.0	-12.0	-37.7	-37.7	-6.6	-13.2	-31.1	37.6
$La_2N@C_{48-q}La$	0.81	-	-1.1	-21.6	-	-	-40.7	-19.3	-	-	-0.6	-23.6	-	-
C_{48-q}	-2.9	-	-2.9	-3.0	-	-	-2.8	3.1	-	-	-2.8	-3.1	-	-
C_{60-q}	-	15.8	-	-	16.1	16.0	-	-	16.0	16.1	-	-	11.5	19.4

cage for the global aromaticity. A negative value of NICS indicated that the system is aromatic; a positive value corresponds to an anti-aromatic molecule and nonaromatic compounds show a value close to zero. According to our results, C_{48-q} may be considered as non-aromatic and C_{60-q} as anti-aromatic. When trimetallic nitride clusters are encapsulated in C_{48-q}, six molecules become aromatic ($Y_3N@C_{48-q}$, $YSc_2N@C_{48-q}$, $LaSc_2N@C_{48-q}$, $ScY_2N@C_{48-q}$, $ScLa_2N@C_{48-q}$ and $YLa_2N@C_{48-q}$), and consequently, a better electronic delocalization is expected compared to nonaromatic or anti-aromatic systems. In contrast, for the C_{60-q} molecule only three quasi-metallofullerene systems show aromaticity ($LaSc_2N@C_{60-q}$, $LaY_2N@C_{60-q}$ and $ScLa_2N@C_{60-q}$). NICS(1) were computed at 1 Å in each direction with regard to the center of the structure. In all cases, the NICS(1) correspond to high negative values. According to our results, these systems are aromatic, and this may be due to the electron donation from the trimetallic nitride clusters to the carbon cages, as previously reported.[19]

On Table 3, we report the deformation energies (kcal/mol), which indicate the level of stress that the encapsulation of

Table 3. Deformation energies (ΔE_{def}, kcal mol^{-1}) for systems under study.

Molecular system	Deformation energy (kcal/mol)	
	C_{48-q}	C_{60-q}
$Sc_3N@C_{n-q}$	-28.37	-20.49
$Y_3N@C_{n-q}$	-70.85	-35.39
$La_3N@C_{60-q}$	–	-17.56
$YSc_2N@C_{n-q}$	-36.48	-22.81
$LaSc_2N@C_{n-q}$	-53.99	-29.15
$ScY_2N@C_{n-q}$	-52.00	-26.71
$LaY_2N@C_{n-q}$	-81.86	-25.86
$ScLa_2N@C_{n-q}$	-84.57	-22.19
$YLa_2N@C_{n-q}$	-99.12	-20.05
$La_2N@C_{48-q}$-La	-133.24	–

trimetallic nitride cluster inside the carbon cage may be subjected to. The deformation energy for the $Sc_3N@C_{48-q}$ system is smaller than for $La_2N@C_{48-q}$-La (-28.37 kcal/mol vs −133.24 kcal/mol). Moreover, the deformation energies for the

C_{60-q} systems are smaller than those found for the C_{48-q} cluster, which may also be intuitive.

To gain further insight into the trimetallic nitride clusters encapsulated by quasi-fullerenes, we have presented the Frontier Molecular Orbitals (FMOs) (HOMO-1, HOMO, and LUMO) on Figure 6, for the $Sc_3N@C_{48-q}$ and $Sc_3N@C_{60-q}$ systems. We have selected these two systems to carry on this further study since $Sc_3N@C_{48-q}$ is the compound with the most exergonic reaction of the C_{48-q} family. Additionally, the main conclusions of this section are valid for the other systems (See Fig. SM3 and SM4 of Supporting Information).

For both compounds, the orbital distribution of the occupied energy levels is mainly located on the carbon cage. This implies an electrostatic interaction and a possible electron transfer among Sc_3N to C_{48-q} and Sc_3N to C_{60-q}.[54–58] Particularly, at the $Sc_3N@C_{60-q}$ system, the bonding molecular orbital (HOMO-1) shows that the interaction between the trimetallic cluster and C_{60-q} may have a covalent character, due to the mixture of π MOs of the carbon cage and the $3d_{xy}$ of Sc atom. This may be explained by the size difference of the cages and the geometry of Sc_3N inside the cage.

The NBO[59] charges were computed to understand the charge transfer mechanism. The Sc atoms donate 0.987 and 1.076 in $Sc_3N@C_{48-q}$ and $Sc_3N@C_{60-q}$ molecules, respectively. These results indicate that the charge transfer direction is from the Sc atom to carbon cage. Furthermore, the bond between Sc atom and the cage has an important ionic character. The NBO results are in agreement with the Frontier Molecular Orbital previously analyzed.

On the other hand, the total density of states (DOS) and partial density of states (PDOS) of the $Sc_3N@C_{48-q}$ (Figure 7.a) and $Sc_3N@C_{60-q}$ (Figure 7.b) systems were calculated to explore the electronic changes due to the presence of Sc_3N clusters. As it may be expected, the presence of Sc atoms contribute to the generation of new electronic states. Those results are in agreement with the FMO analysis and the NBO charges interpretation, since there is a charge transfer from the trimetallic nitride cluster to the carbon cage.
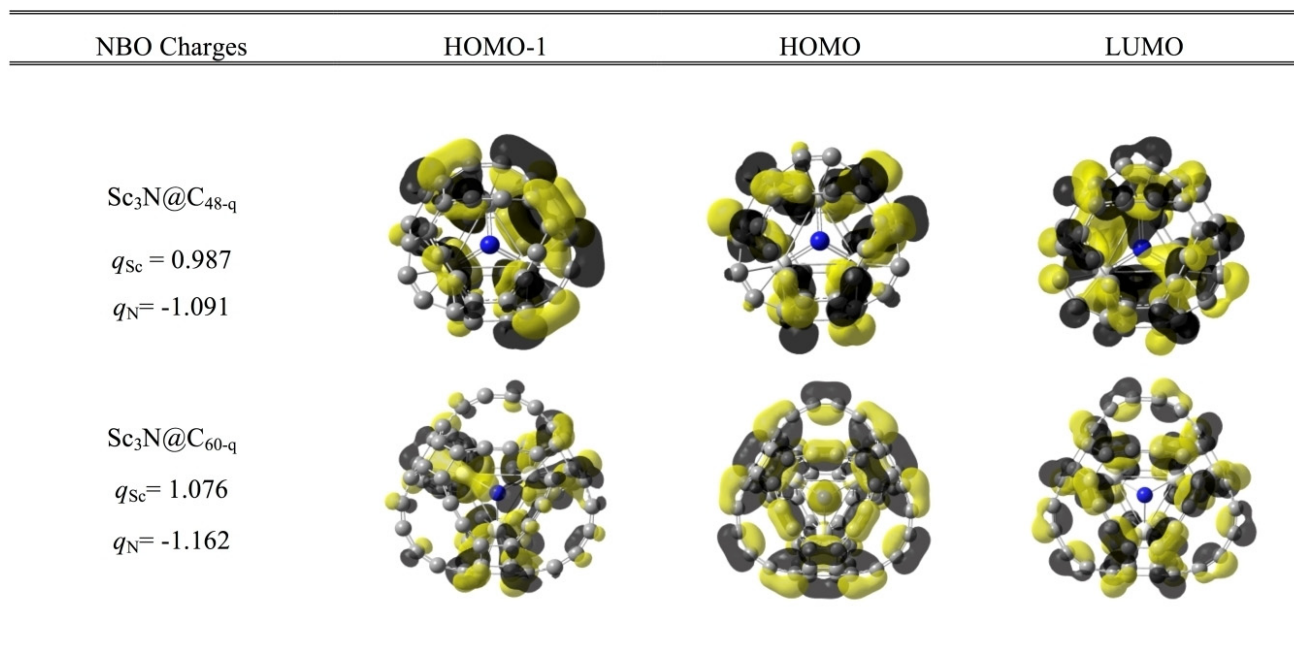
NBO Charges	HOMO-1	HOMO	LUMO
$Sc_3N@C_{48-q}$ $q_{Sc} = 0.987$ $q_N = -1.091$			
$Sc_3N@C_{60-q}$ $q_{Sc} = 1.076$ $q_N = -1.162$			

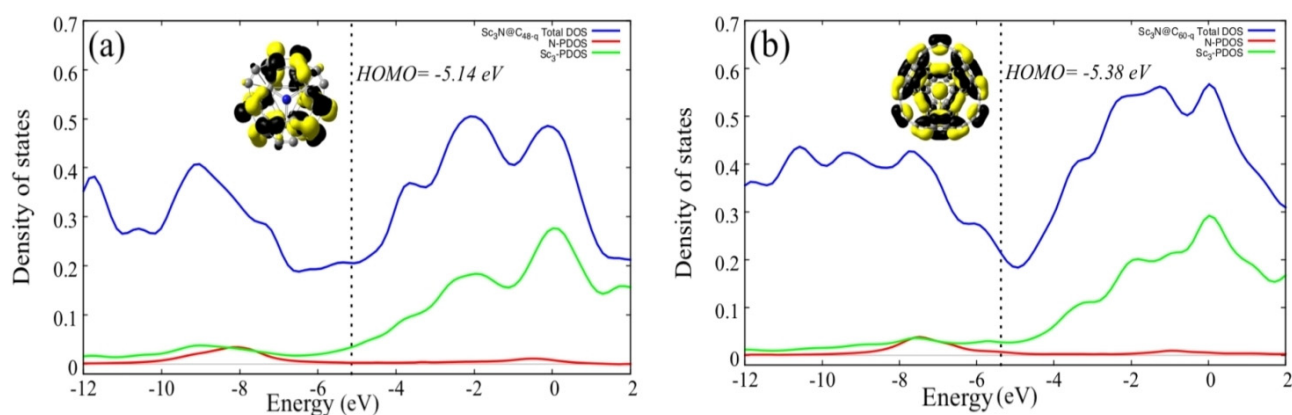**Figure 6.** Frontier Molecular Orbitals (MOs) of $Sc_3N@C_{48-q}$ and $Sc_3N@C_{60-q}$, q_{Sc} and q_N stands for NBO charges of Sc and N.

Figure 7. Total and partial density of states and selected frontier orbitals (a) $Sc_3N@C_{48-q}$ and (b) $Sc_3N@C_{60-q}$.

Single Electron Transfer Mechanism

SET mechanism for the quasi-fullerenes C_{48-q} and C_{60-q} and for quasi-metallofullerenes was investigated in order to examine if donor acceptor properties are enhanced due to presence of trimetallic nitride clusters. In Figure 8, we report the FEDAM. Systems located down to the left are better electron donors but worse electron acceptor compared to those found up to the right.

C_{60-q} is better electron donor-acceptor system than C_{48-q} cluster is, since it has a lower I value and a greater A value. Comparing C_{48-q} to $A_3N@C_{48-q}$ and $A_{3-x}B_xN@C_{48-q}$ systems, it clearly appears that quasi-metallofullerenes are in all cases better electron donor molecules, and in most of the cases (the only exception is $La_3N@C_{48-q}$) better electron acceptor com-

pounds. The C_{60-q} system compared to $A_3N@C_{48-q}$ and $A_{3-x}B_x N@C_{48-q}$ molecules shows that systems containing metals are better electron donors (I values are smaller) but the electron acceptor capacity is decreased (smaller A values). In summary, the presence of trimetallic nitride clusters enhances donor properties of quasi-fullerenes under study. Nevertheless, the capacity to accept an electron is not present at all cases.

Thermal stability

Thermal stability on the compounds has been analyzed by selecting the $Sc_3N@C_{48-q}$ and $Sc_3N@C_{60-q}$ systems, due to the properties previously on this work. Figure 9 shows the ADMP molecular dynamics profile of the potential energy surface, which was calculated with 500 steps of a 1 fs at a temperature
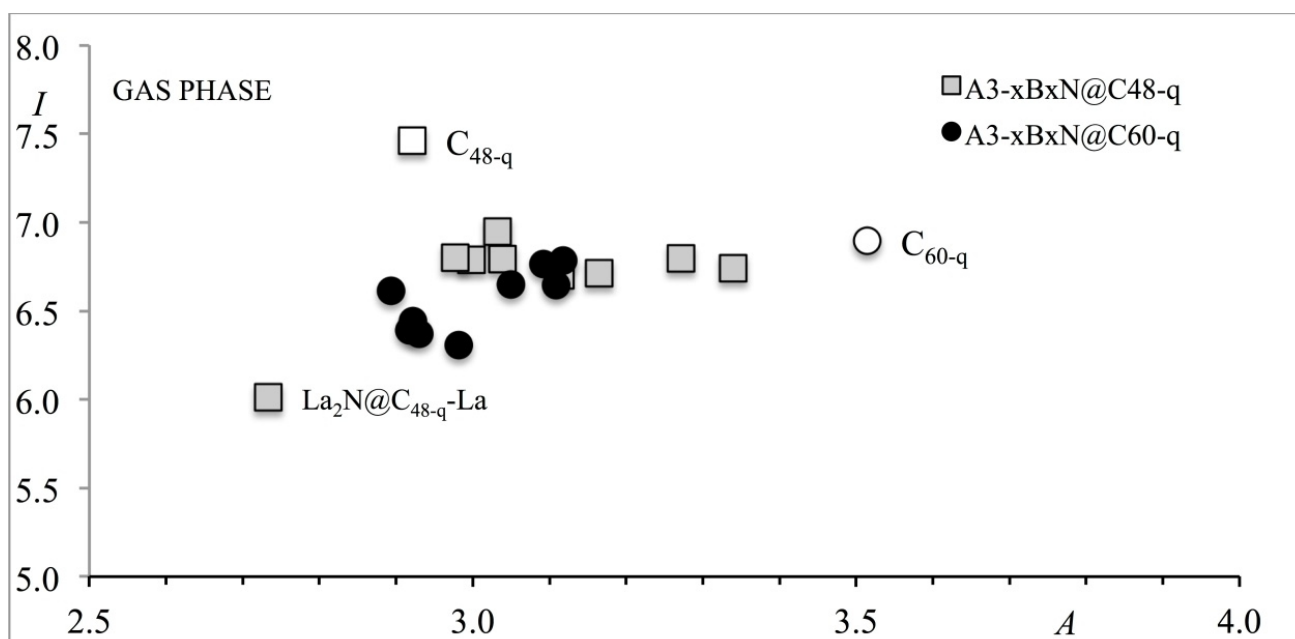
Figure 8. FEDAM for $A_3N@C_{n-q}$ and $A_{3-x}B_xN@C_{n-q}$ (A, B = Sc, Y and La, x = 0-3 and n = 48 and 60).
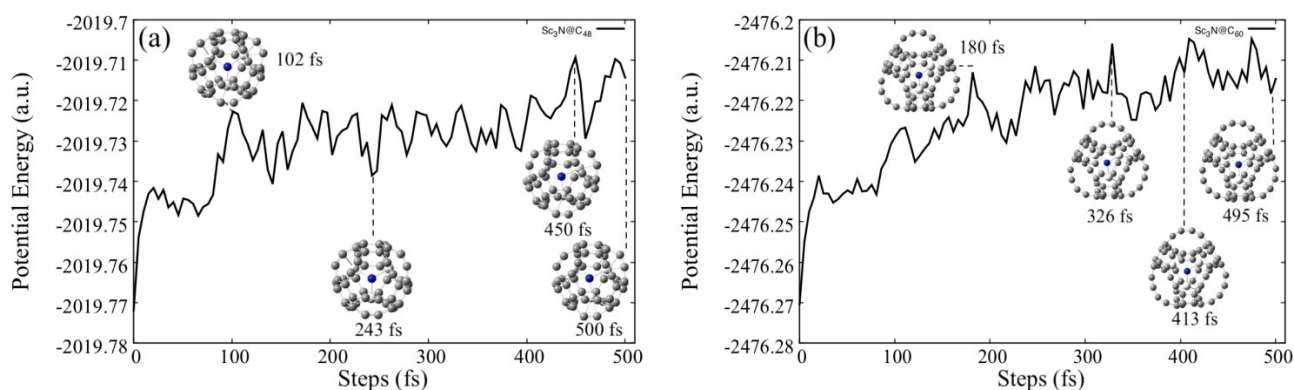

Figure 9. ADMP molecular dynamics profile of potential energy surface (PES) computed with PBE/LanL2DZ level for (a) $Sc_3N@C_{48-q}$ and (b) $Sc_3N@C_{60-q}$ (Temperature ramp T_1 = 800 K to T_2 = 4000 K).

ranging from 800 to 4000 K. These parameters are in agreement to previous works, in which structure stability of small endohedral metallofullerenes has been analyzed, and the study of stability of new buckyball type species.[58,60]

Molecular dynamics were performed from ground state structures obtained with DFT. In both diagrams, the potential energy ranges from 0.02 to 0.06 a.u. (0.54 – 1.63 eV). The $Sc_3N@C_{48-q}$ shows important variations in the following bond lengths: length d_{N-Sc} = 2.00–1.95 Å, d_{C-C} = 1.28–1.30 Å and d_{Sc-C} = 2.30–2.20 Å. The elongation of these bond lengths occurs at 102, 245 and 450 fs. In the case of $Sc_3N@C_{60-q}$ system, we found a slight difference in bond lengths during the simulation with d_{N-Sc} = 2.00–1.93 Å, d_{C-C} = 1.28–1.27 Å and d_{Sc-C} = 2.30–2.31 Å for the 180, 326 and 413 fs, respectively. In both cases, the chemical bonds of the quasi-fullerenes are not broken and they only present a slight ring deformation. Additionally, there is no

bond breaking in the Sc_3N clusters. Thus, both compounds showed a high stability. These results are important since the thermal stability opens the possibility of synthesis in the laboratory, using methods that requiring high temperatures (4000 K) as a condition.

Figure 10 presents an additional study of thermal stability, which was carried out with semi empirical PM6 method to elucidate the evolution of the systems $Sc_3N@C_{48-q}$ and $Sc_3N@C_{60-q}$ subjected to the same temperature regime with a longer time: 1000 fs. Results show a considerable structural deformation in the carbon cages before 1000 fs. At 121 fs, the breaking of the carbon cage is occurring for the $Sc_3N@C_{48-q}$ system. The deformation is even more significant after 434 fs, where the Sc_3N cluster is also broken. Finally, it in can be seen that after 855 fs, there is no structural stability in the molecule. Meanwhile, the $Sc_3N@C_{60-q}$ system presents structural deforma-
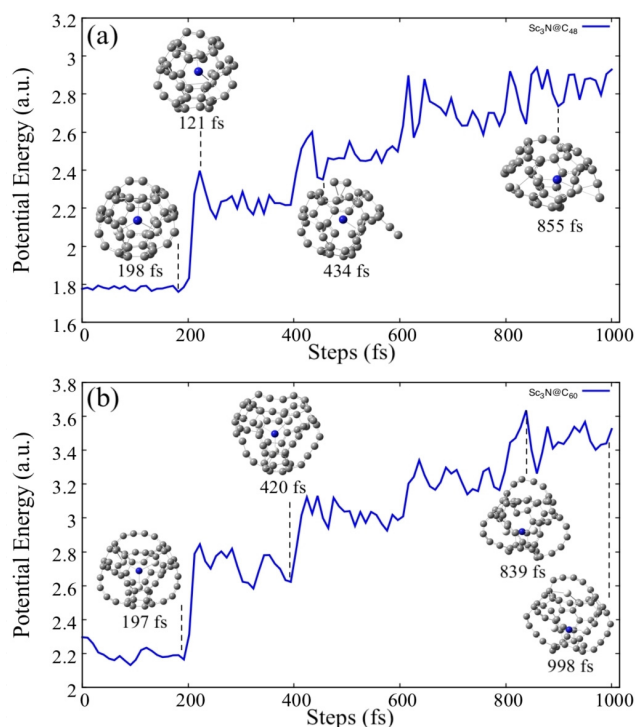
Figure 10. ADMP molecular dynamics profile of the potential energy surface (PES) calculated with PM6 method (a) $Sc_3N@C_{48-q}$ and (b) $Sc_3N@C_{60-q}$ (Temperature ramp $T_1 = 800$ K to $T_2 = 4000$ K).

Conflict of Interest

The authors declare no conflict of interest.

tions, but without losing its spherical shape before 839 fs. At 998 fs, the C_{60-q} carbon cage is strongly deformed and the Sc—N bonding is broken. According to our results, only the C_{60-q} systems present a high thermal stability.

Conclusions

Small C_{48-q} and C_{60-q} systems are thermodynamically capable of encapsulating different trimetallic nitride clusters. In all cases, ΔG energy values correspond to exergonic reactions, and thus the formation of the quasi-metallofullerenes is thermodynamically favored. Moreover, by analyzing the Frontier Molecular Orbitals diagrams and the NBO charges, we corroborated that these systems are stabilized by the charge transfer from trimetallic nitride cluster to the hollow carbon cage. Additionally, the chemical stability is enhanced due to the presence of clusters. According to our results, the capacity of the $A_{3-x}B_x$ $N@C_{n-q}$ systems to donate an electron is always enhanced when is compared to the bare quasi-fullerenes; and in some cases, the capability to accept an electron is also increased. Furthermore, our ADMP molecular dynamics study confirms that these systems (specially C_{60-q}) show an important thermal stability. This may also be important as guidance to experimentalists, since the synthesis may be carried out at high temperatures.

[1] H. W. Kroto, J. R. Heath, S. C. O'Brien, R. F. Curl, R. E. Smalley, *Nature* **1985**, *318*, 162–163.
[2] A. A. Popov, S. Yang, L. Dunsch, *Chem. Rev.* **2013**, *113*, 5989–6113.
[3] S. Nagao, T. Kurikawa, K. Miyajima, A. Nakajima, K. Kaya, *J. Phys. Chem. A* **1998**, *102*, 4495–4500.
[4] S. Stevenson, G. Rice, T. Glass, K. Harich, F. Cromer, M. R. Jordan, J. Craft, E. Hadju, R. Bible, M. M. Olmstead, K. Maitra, A. J. Fisher, A. L. Balch, H. C. Dorn, *Nature* **1999**, *401*, 55–57.
[5] L. Dunsch, S. Yang, *Small* **2007**, *3*, 1298–1320.
[6] H. Shinohara, *Rep. Prog. Phys.* **2000**, *63*, 843–892.
[7] M. N. Chaur, F. Melin, A. L. Ortiz, L. Echegoyen, *Angew. Chem. Int. Ed.* **2009**, *48*, 7514–7538; *Angew. Chem.* **2009**, *121*, 7650–7675.
[8] M. Murata, Y. Murata, K. Komatsu, *Chem. Commun.* **2008**, *46*, 6083–6094.
[9] M. A. Gabriel, L. Genovese, G. Krosnicki, O. Lemaire, T. Deutsch, A. A. Franco, *Phys. Chem. Chem. Phys.* **2010**, *12*, 9406–9412.
[10] M. Takata, B. Umeda, E. Nishibori, M. Sakata, Y. Saitot, M. Ohno, H. Shinohara, *Nature* **1995**, *377*, 46–49.
[11] O. V. Oliveira, A. S. Gonçalves, *Comput. Chem.* **2014**, *2*, 51–58.
[12] J. Chen, Z. Qin, J. Pan, M. Huang, S. Du, G. Cao, *Langmuir* **2015**, *31*, 11438–11442.
[13] D. Soto, R. Salcedo, *Molecules* **2012**, *17*, 7151–7168.
[14] P. W. Dunk, M. Mulet-Gas, Y. Nakanishi, N. K. Kaiser, A. Rodríguez-Fortea, H. Shinohara, J. M. Poblet, A. G. Marshall, H. W. Kroto, *Nature Commun.* **2014**, *5*, 1–8.
[15] R. Salcedo, *Polyhedron* **2015**, *99*, 177–185.
[16] R. Salcedo, *Polyhedron* **2009**, *28*, 431–436.
[17] A. Miralrio, L. E. Sansores, *Comput. Theor. Chem.* **2016**, *1083*, 53–63.
[18] E.-B. Andrade, A. Martínez, *Comput. Theor. Chem.* **2017**, *1115*, 127–135.
[19] A. Miralrio, L. E. Sansores, *Int. J. Quantum. Chem.* **2017**, *117*, e25335.
[20] S. Dhiman, R. Kumar, K. Dharamvir, *J. Mol. Struct.* **2015**, *1100*, 328–337.

[21] L. Dunsch, S. Yang, *Electrochem. Soc. Interface* **2006**, *15*, 34–39.

[22] J. R. Heath, S. C. O'Brien, Q. Zhang, Y. Liu, R. F. Curl, H. W. Kroto, F. K. Tittl, R. E. Smalley, *J. Am. Chem. Soc.* **1985**, *107*, 7779–7780.

[23] Y. Chai, T. Guo, C. Jin, R. E. Haufler, L. P. F. Chibante, J. Fure, L. Wang, G. M. Alford, R. E. Smalley, *J. Phys. Chem.* **1991**, *95*, 7564–7568.

[24] H. Shinohara, *Rep. Prog. Phys.* **2000**, *63*, 843–892.

[25] J. Zhang, S. Stevenson, H. C. Dorn, *Acc. Chem. Res.* **2013**, *46(7)*, 1548–1557.

[26] M. V. Ryzhkov, B. Delley, *Comput. Theor. Chem.* **2013**, *1013*, 70–77.

[27] S. Yang, M. Kalbac, A. Popov, L. Dunsh, *Chem. Phys. Chem.* **2006**, *7*, 1990–1995.

[28] Y. Liduka, O. Ikenaga, A. Sakuraba, T. Wakahara, T. Tsuchiya, Y. Maeda, T. Nakahodo, T. Akasaka, M. Kako, N. Mizorogi, S. Nagase, *J. Am. Chem. Soc.* **2005**, *127*, 9956–9957.

[29] S. Li, C. Tang, X. Zhang, *Comput. Theor. Chem.* **2016**, *1084*, 17–24.

[30] J. U. Reveles, N. N. Karle, T. Baruah, R. R. Zope, *J. Phys. Chem. C* **2016**, *120*, 2603–26092.

[31] Y. Zhan, K. B. Ghiassi, Q. Deng, N. A. Samoylova, M. M. Olmstead, A. L. Balch, A. A. Popov, *Angew. Chem. Int. Ed.* **2015**, *54*, 495–499; *Angew. Chem.* **2015**, *127*, 505–509.

[32] J. U. Reveles, T. Heine, A. K. Köster, *J. Phys. Chem. A* **2005**, *109*, 7068–7072.

[33] X. Lu, T. Akasaka, S. Nagase, *Chem. Commun.* **2011**, *47*, 5942–5957.

[34] A. Rodríguez-Fortea, A. L. Balch, J. M. Poblet, *Chem. Soc. Rev.* **2011**, *40*, 3551–3563.

[35] X. Lu, L. Feng, T. Akasaka, S. Nagase, *Chem. Soc. Rev.* **2012**, *41*, 7723–7760.

[36] P. P. Fatouros, F. D. Corwin, Z. J. Chen, W. C. Broaddus, J. L. Tatum, B. Kettenmann, Z. Ge, H. W. Gibson, J. L. Russ, A. P. Leonard, J. C. Duchamp, H. C. Dorn, *Radiology* **2006**, *240*, 756–764.

[37] M. Ehrich, R. Van Tassell, Y. B. Li, Z. G. Zhou, C. L. Kepley, *Toxicol. Vitro* **2011**, *25*, 301–307.

[38] M. Liedtke, A. Sperlich, H. Kraus, A. Baumann, C. Deibel, M. J. M. Wirix, J. Loos, C. M. Cardona, V. Dyakonov, *J. Am. Chem. Soc.* **2011**, *133*, 9088–9094.

[39] L. Feng, M. Rudolf, S. Wolfrum, A. Troeger, Z. Slanina, T. Akasaka, S. Nagase, N. Martin, T. Ameri, C. J. Brabec, D. M. Guldi, *J. Am. Chem. Soc.* **2012**, *134*, 12190–12197.

[40] E. W. Godly, R. Taylor, *Pure & Appl. Chem.* **1997**, *69(7)*, 1411–1434.

[41] L. H. Gan, J. Q. Zhao, F. Pan, *J. Mol. Struct.: THEOCHEM* **2010**, *953*, 24–27.

[42] V. V. Pokropivny, A. L. Ivanovskii, *Russ. Chem. Rev.* **2008**, *77(10)*, 837–873.

[43] A. Hirsch, *Nature Materials* **2010**, *9(11)*, 868–871.

[44] O. Kharlamov, M. Bondarenko, G. Kharlamova, V. Fomenko, Springer Netherlands, **2015**, pp. *191–205*.

[45] A. I. Kharlamov, G. A. Kharlamova, M. E. Bondarenko, *Russ. J. Appl. Chem.* **2013**, *86(8)*, 1174–1183.

[46] A. I. Kharlamov, M. E. Bondarenko, G. A. Kharlamova, V. V. Fomenko, Proceedings of the International Conference Nanomaterials: Applications and Properties, vol. 4(2), **2015**, 02NEA01(4pp).

[47] L. Tang, L. Sai, J. Zhao, R. Qiu, *Comput. Theor. Chem.* **2011**, *969*, 35–43.

[48] E. F. Kustov, V. I. Nefedov, A. V. Kalinin, G. S. Chernova, *Russ. J. Inorg. Chem.* **2008**, *53(9)*, 1384–1395.

[49] C. A. Celaya, J. Muñiz, L. E. Sansores, *Comput. Theor. Chem.* **2017**, *1117*, 20–29.

[50] M. Feyereisen, M. Gutowski, J. Simons, J. Almlöf, *J. Chem. Phys.* **1992**, *96*, 2926–2932.

[51] L. H. Gan, J. Q. Zhao, Q. Hui, *J. Comput. Chem.* **2010**, *31(8)*, 1715–1721.

[52] N. B. Shustova, A. A. Popov, M. A. Mackey, C. E. Coumbe, J. P. Phillips, S. Stevenson, S. H. Strauss, O. V. Boltalina, *J. Am. Chem. Soc.* **2007**, *129*, 11676–11677.

[53] J. M. Campanera, C. Bo, M. M. Olmstead, A. L. Balch, J. M. Poblet, *J. Phys. Chem A* **2002**, *106*, 12356–12364.

[54] E. V. Shah, D. R. Roy, *Physica E Low Dimens. Syst. Nanostruct.* **2015**, *70*, 157–164.

[55] E. V. Shah, D. R. Roy, *Physica E Low Dimens. Syst. Nanostruct.* **2016**, *84*, 354–360.

[56] Z. Mahdavifar, M. Ershadifar, A. Farrokhnia, *J. Electron. Mater.* **2018**, *47*, 550–565.

[57] A. L. Svitova, A. A. Popov, L. Dunsch, *Inorg. Chem.* **2013**, *52*, 3368–3380.

[58] M. M. Gas, L. Abella, P. W. Dunk, A. Rodríguez-Fortea, H. W. Kroto, J. M. Poblet, *Chem. Sci.* **2015**, *6*, 675–686.

[59] E. D. Glendening, A. E. Reed, J. E. Carpenter, F. Weinhold, NBO Version 3.1.

[60] G. M. Guajardo, J. L. Cabellos, A. D. Celaya, S. Pan, Rafael Islas, P. K. Chattaraj, T. Heine, G. Merino, *Sci. Rep.* **2015**, *05*, 11287.